Untargeted Tear Proteomics in a Large South-Asian Cohort Reveals Inflammatory Signaling, ECM Remodeling, and Altered Metabolism in Keratoconus

Ramaraj Kannan,[1,2] Rohit Shetty,[2,3] Trailokyanath Panigrahi,[1] Siew Kwan Koh,[4] Pooja Khamar,[3] Vrushali Deshpande,[1] Rudy M. M. A. Nuijts,[2] Marlies Gijs,[2] Krishnatej Nishtala,[1] Lei Zhou,[5,6] and Arkasubhra Ghosh[1]

[1]GROW Research Laboratory, Narayana Nethralaya Foundation, Narayana Nethralaya Eye Hospital, Bangalore, Karnataka, India
[2]University Eye Clinic Maastricht, School for Mental Health and Neuroscience, Maastricht University, Maastricht, The Netherlands
[3]Department of Cornea and Refractive Surgery, Narayana Nethralaya, Bengaluru, Karnataka, India
[4]Ocular Proteomics, Singapore Eye Research Institute, Singapore, Singapore
[5]School of Optometry, Department of Applied Biology and Chemical Technology, Research Centre for SHARP Vision (RCSV), The Hong Kong Polytechnic University, Hung Hom, Kowloon, Hong Kong
[6]Centre for Eye and Vision Research (CEVR), Hong Kong

Correspondence: Arkasubhra Ghosh, GROW Research Laboratory, Narayana Nethralaya Foundation, Narayana Nethralaya, Bengaluru, Karnataka 560099, India; arkasubhra@narayananethralaya.com. Lei Zhou, School of Optometry, Department of Applied Biology and Chemical Technology, Research Centre for SHARP Vision (RCSV), The Hong Kong Polytechnic University, Hung Hom, Kowloon 100 HKD, Hong Kong; lei.henry.zhou@polyu.edu.hk.

Received: October 30, 2024
Accepted: January 28, 2025
Published: February 24, 2025

Citation: Kannan R, Shetty R, Panigrahi T, et al. Untargeted tear proteomics in a large South-Asian cohort reveals inflammatory signaling, ECM remodeling, and altered metabolism in keratoconus. *Invest Ophthalmol Vis Sci.* 2025;66(2):60. https://doi.org/10.1167/iovs.66.2.60

Purpose. Keratoconus (KC), a progressive corneal degenerative disease, is characterized by focal thinning and weakening, and the molecular pathways driving such changes are still being discovered. The progression-related pathologic molecular factors have not been identified in genetic studies from KC, and stage-specific molecular changes remain unknown in prior protein studies. We address this challenge through untargeted mass spectrometry analysis in a large KC cohort.

Methods. The cohort comprised 40 healthy individuals and 107 eyes with varying KC grades from 69 individuals. Quantitative proteomics using iTRAQ labeling coupled with two-dimensional nanoLC-ESI-MS/MS (TripleTOF 5600) was employed followed by validation.

Results. Unbiased LC-MS/MS analysis identified 1104 proteins, with 279 quantified proteins. Thirty-two proteins exhibited significant dysregulation in tear fluids compared to the control, enriched in glycolytic pathways, extra-cellular matrix (ECM) organization, reactive oxygen detoxification, and inflammatory regulation. Cystatin-S, lacritin, glutathione synthetase, and superoxide dismutase were validated to have differential expression across each KC grade.

Conclusions. Our data unveiled novel tear fluid proteins involved in unique biological processes such as neutrophil degranulation, autophagy, metabolic alterations, protein phosphorylation, and more, apart from the ECM modulation and inflammatory pathways. Although the newly identified progressive KC biomarkers will help in disease characterization, identified molecular pathways may serve as novel therapeutic targets.

Keywords: keratoconus, proteomics, ECM, tears, molecular networks

Keratoconus (KC) is a bilateral and asymmetric corneal disease characterized by focal structural changes, resulting in progressive thinning, biomechanical weakening, and steepening of the cornea that can lead to loss of visual acuity because of irregular astigmatism and corneal scarring in more advanced cases.[1] Clinical diagnosis of KC is done by measuring corneal topography, a noninvasive imaging technique to identify the posterior curvature of the cornea and the thickness distribution that informs about disease stage.[2] People of all ethnicities and genders are affected by this disease, but the prevalence and incidence vary among ethnicities and geographical locations.[3] The estimated prevalence rates of KC globally were found to be between 0.2 and 4790 per 100,000 individuals, and the incidence rate varies between 1.5 and 25 cases per 100,000 individuals/year. The highest rate of KC has been reported in Middle Eastern and Asian ethnicities aged 20 to 30 years old.[3] In the United States alone the prevalence was estimated to be 0.15% with different age groups.[4] KC was primarily believed to be a noninflammatory corneal degenerative disease because of the lack of evidence on corneal inflammation and immune cell infiltration. However, recent developments in understanding the disease have witnessed increased inflammatory factors and immune cells either at the site of the disease or

in the systemic circulation in cases of KC patients, revising the classical concept of noninflammatory disease.[1,5,6]

Despite the intense research on KC pathogenesis, the exact cause of the disease is not conclusive. Multiple etiological factors including biomechanical, environmental, and genetics play a role in developing KC.[7,8] The critical changes happen in all the layers of the cornea. With KC progression, corneal epithelial cells and keratocytes are affected. Epithelium degeneration, irregular epithelial surface, thinning of the central cornea, and reduced stromal keratocyte numbers have been reported in KC corneas.[9–11] Altered expression and arrangement of extracellular matrix protein components like collagen, and proteoglycans in the stromal layer occur in KC.[11,12] A decreasing trend in the collagen crosslinking enzyme LOX levels and enzymatic activity in tear fluids were observed in higher grades of KC.[13–16] Similarly, by modulating collagen degradation proteolytic enzymes like collagenase, gelatinase, peptidase, and heparinase play a major role in extra-cellular matrix (ECM) remodeling. These enzyme activities are reported to be higher in case of KC patients.[17–19] Other enzymes like Cathepsin B and G levels are high in KC patients.[17,20] Proteolytic enzymes such as matrix metalloproteinases (MMP) 9 and 2 were found to be high in cornea and tear samples of KC patients and a decreased level of major proteinase inhibitors like alpha 1 protease inhibitor, alpha2- macroglobulin and tissue inhibitor of matrix metalloproteinases-1 (TIMP1) were significantly lower in KC patients.[13,21–25] External factors like eye rubbing, contact lens use, and exposure to ultraviolet light induce ocular surface change and trigger the production of inflammatory factors. Recent findings on oxidative stress status in tear fluids, corneal tissue, and serum from KC patients have given evidence that oxidative stress is one of the causative factors for the development of KC and its progression.[26–30] Antioxidant factors like glutathione, heme oxygenase, superoxide dismutase, and heat shock protein 27 were found to be reduced in KC patients, with an increase in inducible nitric oxide synthase, glutathione S-transferase in KC corneas.[31–34]

Tear fluids are an easily accessible body fluid that could be used in biomarker studies to detect the molecular changes happening in a disease condition.[35–37] Tear proteomics has been used in cancer research to find potential biomarkers, identification of tear proteases and study patients' responses to fungal keratitis.[38] Proteomic studies involving different samples from corneal layers, tear film, and aqueous humor have provided fundamental information to understand the event that happens during KC development.[38–44] Tear proteomics data generated from KC patients has shown altered proteins belonging to families of proteases, inflammatory cytokines, cell adhesion molecules, glycoproteins, and transporters as compared to the control samples.[17,38,45–47] In recent shotgun tear proteomic study including normal individuals and KC patients identified dysregulation of proteins involved in iron transport, oxidative stress, protease inhibition along with inflammatory factors.[41] Proteomic studies on isolated epithelia and stroma from KC patients revealed an altered expression of cytokeratin, cytoskeletons, matrix components, and regulatory proteins. Similarly, recent publication on KC proteomics using epithelium and stroma from topologically abnormal cone and non-cone areas revealed that the KC-associated proteome change is not restricted to the diseased cone area but also is found in non-cone areas with normal topology.[8] All the above studies include small patient cohorts, and the comparisons were performed among KC patients and normal individuals, resulting in datasets with limited overlaps. Furthermore, although earlier proteomic analyses have captured the molecular changes in KC, none of the studies have analyzed clinical grade-wise mapping of the disease progression. Hence, the objective of our study is to map the clinically relevant grade-specific molecular changes to understand the biology of KC progression. We further validate the dysregulated proteins in an independent cohort toward identification of effective molecular biomarkers that can provide a framework to assign diagnostic relevance and therapeutic intervention points.

Material and Methods

Study Participants

The observational cohort study, approved by the Narayana Nethralaya Institutional Review Board (ref. no. C/2015/05/05), was conducted in accordance with the Indian Council for Medical Research guidelines and the principles of the Declaration of Helsinki. The sample size estimation was performed based on the comparison of two means for several proteins altered in prior studies[5,13,17] with the power of 90% and two-tailed alpha of 0.05 using MedCalc v.20.0.5. Using select factor, we further estimated the sample size for each grade from the previous study on KC.[5] A total of 40 healthy volunteers and 69 KC patients were selected after informed written consent and comprehensive clinical evaluation at Narayana Nethralaya Eye Hospital, Bangalore, India, to exclude any ongoing or recent ocular or systemic conditions. Additionally, contact lens wearers were excluded from the study. Further, independent cohort of KC patients grades 1–3/4 ($n = 3$ each) and controls ($n = 3$) were recruited for validation.

Diagnosis and Grading Criteria

The Amsler–Krumeich classification, that defines the stage of KC using biomicroscopy, mean central keratometry reading, spherical and cylindrical refraction change, and corneal thickness,[48,49] was used for the final gradation of the KC stages of all subjects in this study ($n = 107$) clinically classified as Grade 1 ($n = 33$), Grade 2 ($n = 25$), Grade 3 ($n = 21$), and Grade 4 ($n = 28$) and normal healthy controls ($n = 40$).

Tear Fluid Collection and Tear Fluid Protein Extraction

Tear fluids were collected using Schirmer's strips (Conta Care Ophthalmics and Diagnostics, Vadodara, India) from both eyes of 31 KC patients and one eye of 45 KC patients for five minutes without anesthesia. The same procedure was used to collect tear fluids from one eye of 40 healthy individuals. After sample collection the Schirmer's strips were stored at −80°C until further analysis. The total tear protein was extracted by vigorously shaking the 1 mm chopped pieces of Schirmer's strip in 150 µL of 100 mM ammonium bicarbonate for three hours at 4°C. The samples were then spun in a centrifuge at 13.2 K rpm for 20 minutes to separate the strips from the solution, and the supernatants were collected. After extraction, the control samples were pooled. The total protein estimation was carried out by standard Bradford colorimetric assay (ThermoFisher, St. Louis, MO, USA).

ITRAQ-Based Quantitative Proteomic Analysis

All samples were labeled with eight-plex iTRAQ reagents as described in the kit (SCIEX, Framingham, MA, USA). Briefly, 30 µg of tear protein were denatured, reduced, and alkylated and subjected to proteolytic digestion using trypsin at an enzyme-to-protein ratio of 1:15 overnight at 37°C. The iTRAQ agents 113 for control, 114, 115, 116, and 117 for KC tear fluids were added to the samples and incubated for three hours at room temperature. After incubation, the labeled samples were pooled and dried using SpeedVac. Loading buffer 10 µL (0.1% formic acid and 2% acetonitrile in water) was added to the dried sample for reconstitution.

The samples were chromatographically separated on a C18 reverse-phase nano column (SCIEX; NanoLC Trap) with water/acetonitrile gradient over 90 minutes using Eksigent nanoLC coupled to SCIEX 5600+ Triple TOF mass spectrometer. Briefly, the labeled peptides were separated on Eksigent 3C18-CL-120, 3 µm, 120 Å, 350 µm x 0.5 mm 0.075 µm × 150 mm analytical column (SCIEX; ChromXP C18) coupled with Eksigent NanoLC Trap Chrom XP CL- 3 µm, 120 Å, 350 µm × 0.5 mm at a flow rate of 250 nL/min over a gradient of 90 minutes using 95% water, 5% acetonitrile, and 0.1% formic acid as aqueous phase/buffer A and 95% acetonitrile, 5% water, and 0.1% formic acid as organic phase/buffer B. The spectra were acquired in information-dependent acquisition mode with top 20 intense peptides considered for fragmentation. Full-scan MS spectra were acquired in the mass range of 350-1250 m/z with an accumulation time of 200 ms, and tandem mass spectra in information-dependent acquisition mode were acquired in 100 m/z–1800 m/z for 50 ms. The resultant MS files were searched against the Uniprot human database for protein identification using Protein Pilot 4.0

Data Analysis

Grade 3 and Grade 4 were considered as Grade 3 for all the analysis because the protein expression found to be similar in the later grades. The principal component analysis (PCA) was performed using Orange v.3.35.0. The standard scalar normalization was performed before calculating the principal components. The first two principal components were plotted as scatter plot. Proteins identified in at least 50% of the samples per grade of KC (percent observations $\geq$0.5) were considered for further analysis. The python package sklearn (v0.1.3.2) was used to classify the grades based on protein expression level. Furthermore the data was plotted as receiver operating characteristic curve to find the classification between each group. Spearman rank correlation was used to find the association between proteins, followed by the hierarchical clustering of proteins based on Euclidian distance.

The geometric means for each grade of KC were calculated. The mean values >1.2 and <0.8 were considered as dysregulated proteins. Mann-Whitney U-test was used to find the statistical significance across different grades.

GraphPad Prism v.8.0.2, was used to plot volcano plot for differential protein expression analysis among each grade. The protein-wise z-score normalization was performed before plotting heatmap. Circlize package in R was used to generate chord plot to represent the pathway annotation. Seaborn (v0.11.2) python package was used to generate line plot, bar plot, density plot and heatmap.

Functional Enrichment and Pathway Analysis

DAVID functional annotation tool was used to find the biological process, cellular component and molecular function of the identified proteins. And Reactome pathway module in the DAVID was used for the pathway annotation. ClueGO, cytoscape v3.10 module, was used to build the protein-pathway network map.

Validation of Differentially Regulated Proteins by Western Blotting

The tear samples from the validation cohort were processed in a similar fashion as mentioned above. For Western blot analysis, 15 µg total protein was separated on 10% SDS polyacrylamide gel. Two different pre-stained protein markers (Novex Sharp Pre-stained protein standard, Cat. No. LC5800 [ThermoFisher]; Precision Plus Protein Dual Color Standard, Cat. No. 1610374 [Bio-Rad Laboratories, Ann Arbor, MI, USA]) were used for molecular weight estimation. Samples were transferred to 0.45-µm PVDF membranes (Bio-Rad Laboratories) by an electro-blotting technique. The following antibodies were used for the validation of the differentially regulated proteins, Lysozyme (1:50000, Cat no. ab108508, Rabbit monoclonal; Abcam, Cambridge, UK), Glutathione synthetase 1 (1:5000, Cat no. ab133592, Rabbit monoclonal; Abcam), superoxide Dismutase1 (1:5000, Cat no. ab13498, Rabbit polyclonal; Abcam), Cystatin S (1:2000, Cat no. ab151771, Rabbit polyclonal; Abcam), Lacritin (1:1500, Rabbit monoclonal; Santa Cruz Biotechnology, Dallas, TX, USA), Lipocalin-1 (1:1000, Mouse monoclonal; Santa Cruz Biotechnology). The blots were incubated with primary antibodies overnight at 4°C. The blots were washed three times with wash buffer for 15 minutes each and then incubated with secondary antibodies for one hour at room temperature. The relative intensity of each band was determined with the Image J software application (downloaded from nih.gov). Quantification was performed by subtracting background readings from the relative intensity for each sample band followed by normalization of band intensity with the Coomassie-stained gel band intensity.

Results

Clinical Features and Analysis Strategy

The current study included 107 eyes from 69 patients diagnosed with KC (58% male and 42% female, with a mean age of 23.8 ± 6.2) and 40 eyes from 40 healthy controls. The controls were age matched with the cases (60% male and 40% female, with a mean age of 25.4 ± 5.3). No differences were found between age and gender for the affected individuals. Based on the clinical grading, the 107 eyes were classified as Grade 1 (54.5% male and 45.5% female, with a mean age of 26.4 ± 4.1), Grade 2 (58.3% male and 41.7% female, with a mean age of 25.8 ± 3.6), and Grades 3 & 4 (58.6% male and 41.4% female, with a mean age of 25.4±3.4) as detailed in (Figs. 1A–E, Supplementary Table S1). The tear fluids collected from healthy subjects were pooled based on the same concentration (30 µg) after protein extraction. The pooled samples were used as the internal iTRAQ control for all the runs to avoid inter-experimental variability during the relative quantitation.

Investigative Ophthalmology & Visual Science

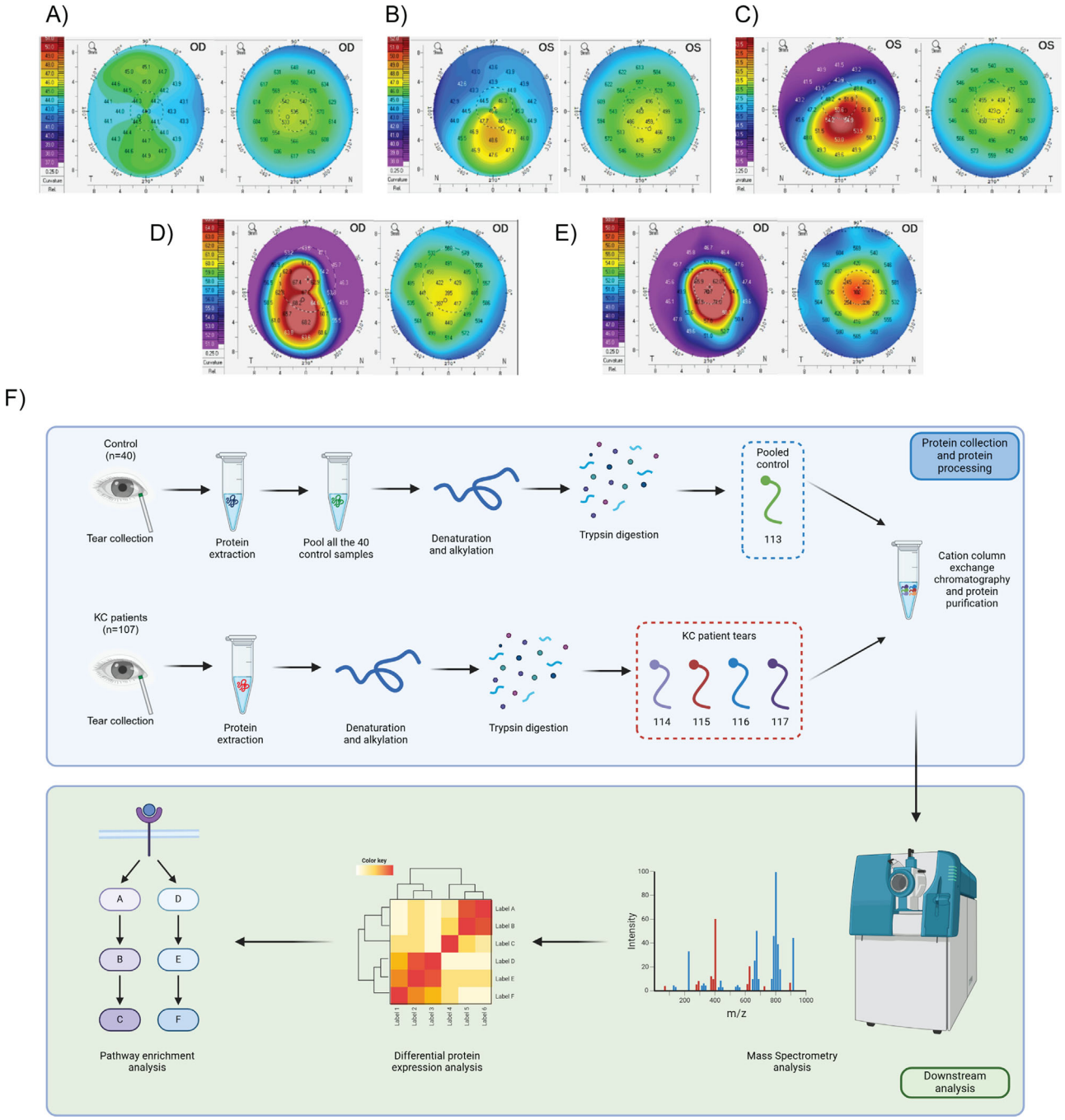

Figure 1. Clinical grading and study overview. Topography of **(A)** a healthy eye, **(B)** Grade 1 KC, **(C)** Grade 2 KC, **(D)** Grade 3 KC, **(E)** Grade 4 KC, and **(F)** tear sample collected from healthy control subjects (n = 40) were pooled after protein extraction and used as iTRAQ control for all the KC tear samples (n = 107). The relative quantitation of the proteins was calculated, and differentially expressed proteins were identified.

Untargeted Protein Identification

Using quantitative proteomic analysis by iTRAQ, 1104 proteins were identified in the tear fluids of patients across different grades of KC. Out of which 279 proteins were quantifiable with unused score >2 and minimum peptide count 2 (Supplementary Table S2). To ensure that the proteins selected for analysis would have application as biomarkers, we selected the proteins that were expressed in the KC samples for at least 50% of the samples per grade. The proteins identified with an observation rate >0.5 in either one of the three grade groups were filtered out, which further cut down to 213 proteins (Fig. 2A). Out of these 213 proteins, 103 proteins had an observation rate >0.8 and 23 proteins identified in all the 107 samples. In addition, we found 66 proteins that had an observation rate < 0.5 in all KC samples. Those proteins show major involvement in extracellular matrix organization, WNT signaling pathway, MAPK signaling cascade, and Rho GTPase signaling (Fig 2A). The functional enrichment showed that the identified 213

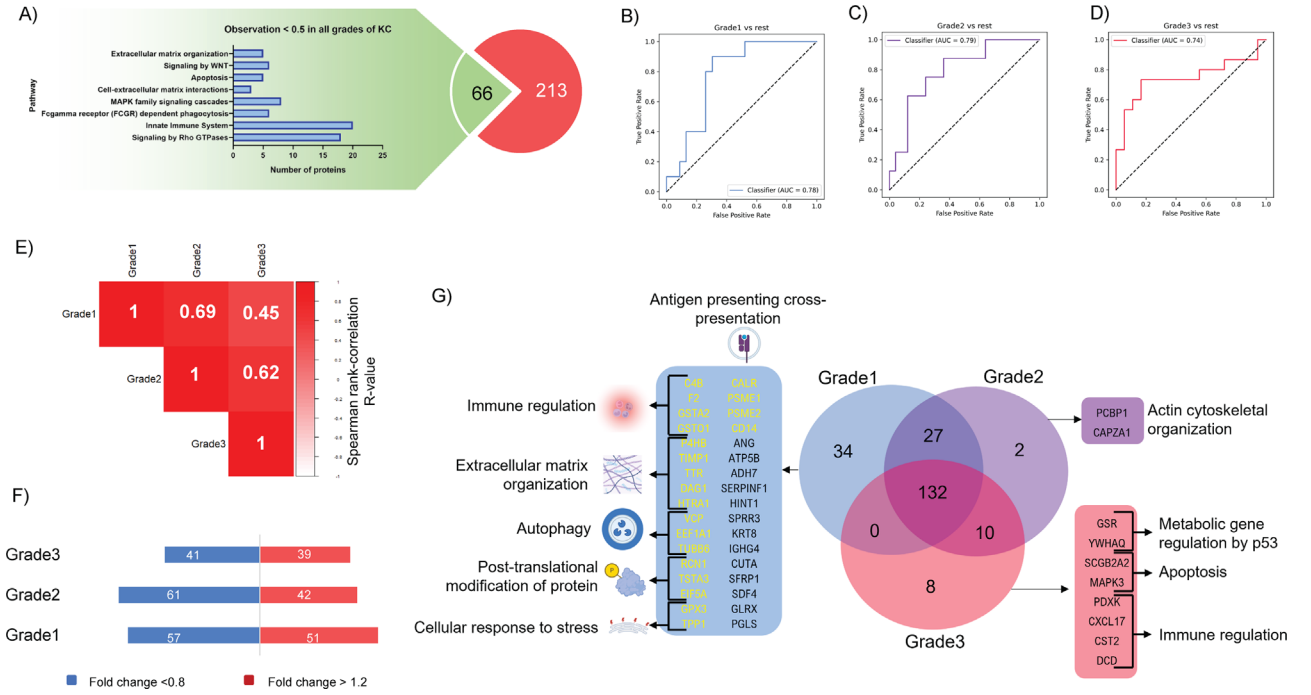

Figure 2. Untargeted protein identification from tear fluid. **(A)** Totally 279 tear proteins were identified with quantitative information in two-peptide range with unused score >2. **(B–D)** Logistic regression classifier predicted AUC curve values 0.78, 0.79, and 0.74 for Grade 1, Grade 2, and Grade 3, respectively, against other grades. **(E)** Spearman correlation heatmap shows the strong positive correlation of Grade 1-Grade 2 and Grade 2-Grade 3. **(F)** *Bar plot* shows the total number of differentially expressed proteins as compared to control. **(G)** Venn diagram illustrates the most abundant expression of proteins in each grades (based on the observation rate [>0.5]).

proteins belong to various biological processes such as the response to inflammation, stress-activated MAPK cascade regulation, redox homeostasis, extracellular matrix degradation, oxidative stress response, and regulation of apoptosis (Supplementary Fig. S1). Most of the secreted proteins are found to be localized in the extracellular and cytoskeletal region (Supplementary Fig. S1). Remarkably, few membrane proteins and nuclear proteins were also identified in the tear fluids.

The relative fold change values of 213 proteins were used for PCA analysis to find the relation between each grade of KC. The PCA plot showed two distinct clusters for Grade 1 and Grade 3 except for a few samples. But Grade 2 did not show any distinct cluster and found it to be spread across Grade 1 and Grade 3 (Supplementary Fig. S2). Further, logistic regression (LR) analysis was carried out to find the classification based on different gradings of KC. Grade 1 was classified against Grade 2 and Grade 3, which showed an AUC value of 0.78 (Fig. 2B). Grade 2 against Grade 1 and Grade 3, Grade 3 against Grade 1 and Grade 2 which got the AUC value of 0.79 and 0.74 respectively (Figs. 2C, 2D). The LR classification showed that ~75% of the protein identification and relative quantitation were true positive to its corresponding group. This shows the differential protein expression is present across different grades of KC. Grade-wise geometric mean values were calculated for all the proteins. Spearman-rank correlation was performed to find the association of proteins across different grades. Grade 1 demonstrates a strong positive correlation ($r = 0.69$) with Grade 2, but weak correlation with Grade 3 ($r = 0.45$). However, Grade 2 showed a positive correlation with Grade 3 ($r = 0.62$) (Fig. 2E). This illustrates the proteome level alterations occurring during disease progression suggesting that pathology may be linked to global changes in protein function in late stages of the disease. Compared to controls, proteins involved in metabolic pathways are downregulated while inflammatory regulatory proteins, proteins involved in ECM degradation are upregulated (Fig. 2F).

Restricting to the observation rate >0.5, common and the higher proportion proteins for each grade were identified (Fig. 2G). Totally 132 proteins were present in all the 3 grades with observation rate >0.5. Thirty-four proteins were found to show a higher proportion in Grade 1. Those proteins are involved in ECM organization, autophagy, PTM of proteins, cellular response to stress, and immune regulation. Two cytoskeletal organization proteins showed higher proportion in Grade 2. Grade 3 showed a higher proportion of eight proteins, which regulate metabolic gene expression by P53 pathway, apoptosis, and inflammation.

Differential Protein Expression Analysis

The 132 proteins that were common to all grades were further considered for differential expression analysis. The major functional pathway enrichment of those proteins revealed altered platelet and neutrophil degranulation, gluconeogenesis, extracellular matrix degradation, metabolic gene regulation, detoxification of reactive oxygen species (ROS), and inflammation (Supplementary Fig. S3A).

The Spearman rank correlation was calculated for each protein (Fig. 3A). Based on the Euclidean distance between the correlation coefficient values, five distinct clusters were formed (Fig. 3A). All five clusters were formed with varying protein numbers (Supplementary Fig. S3B, Supplementary

Investigative Ophthalmology & Visual Science

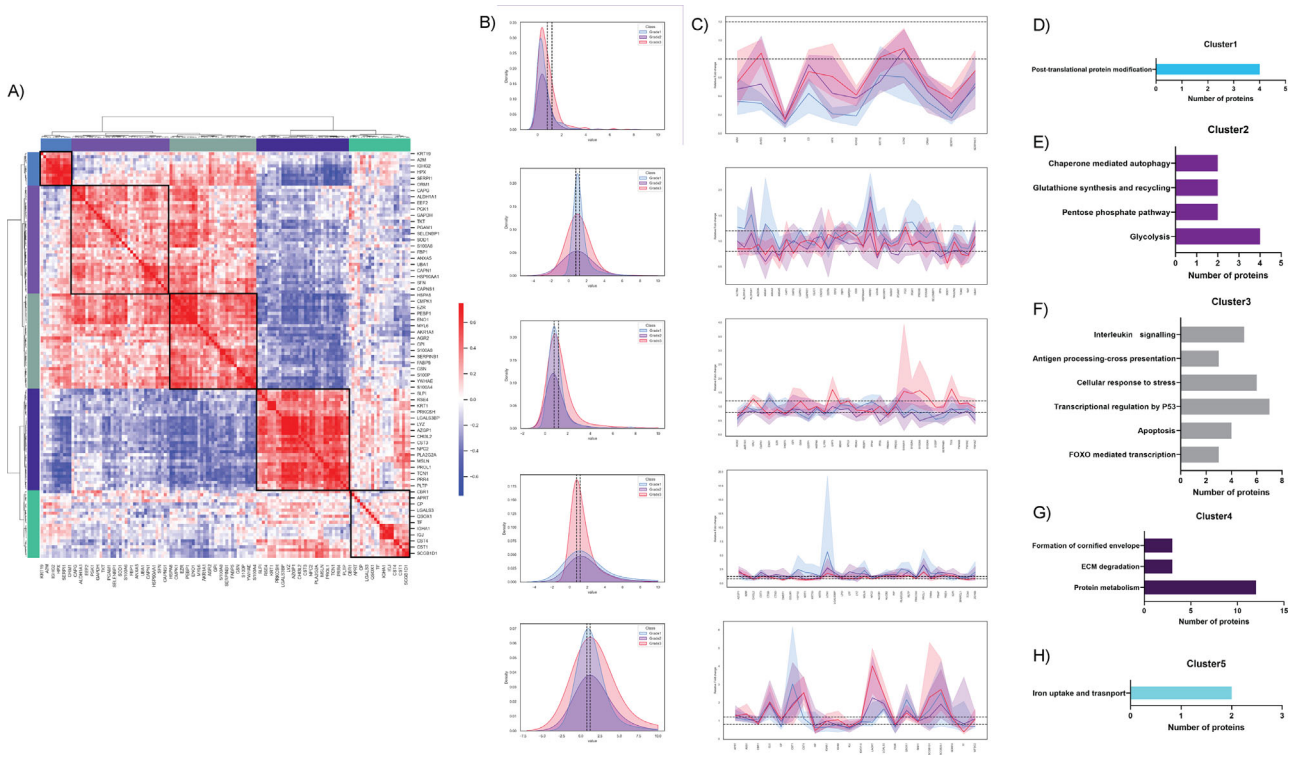

Figure 3. Differential protein expression analysis. **(A)** The heatmap shows the Spearman rank correlation *R*-value for each protein, which were further clustered based on the Euclidian distance. **(B)** Density plot shows the distribution of the majority of the proteins in the particular cluster. Cluster 1, Cluster 3, and Cluster 4 showed distribution away from the center point. **(C)** Line plot shows the list of proteins falling in the particular cluster and its relative expression value as compared to control. **(D–H)** Unique pathway enriched for Cluster 1, Cluster 2, Cluster 3, Cluster 4 and Cluster 5, respectively.

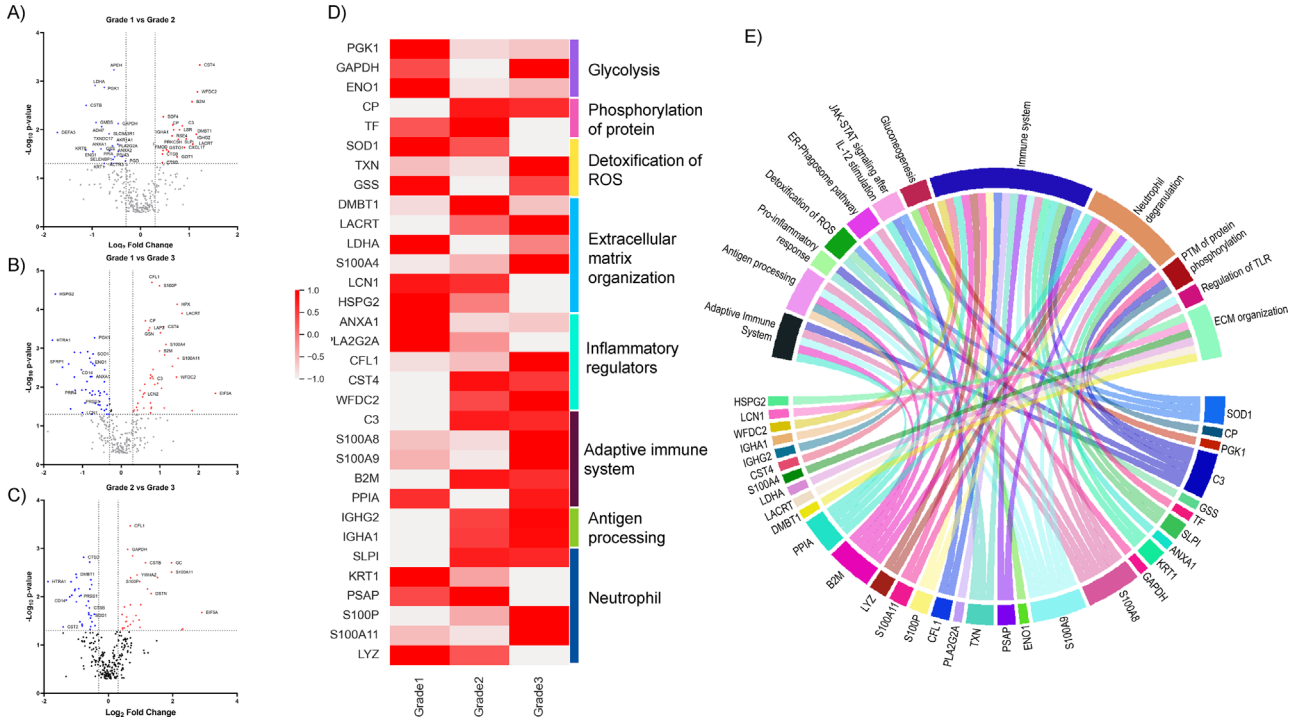

Figure 4. Dysregulation of proteins among different grades of KC. **(A–C)** Volcano plot shows the significantly differential protein expression values of Grade 1 versus Grade 2, Grade 1 versus Grade 3, and Grade 2 versus Grade 3. Mann-Whitney U-test was used to find the statistical significance. The relative fold change value >1.2 was considered as upregulation and <0.8 was considered as downregulation. **(D)** The heatmap shows the expression pattern of 32 major dysregulated proteins across different grades and their major biological functions. **(E)** Chord plot shows the Reactome pathway annotation of the 32 dysregulated proteins.

Table S3). The density plot shows that the dysregulation of proteins was primarily present in Cluster 1, Cluster 3, and Cluster 4, since the density peak is distributed or observed above and below the cutoffs (0.8 and 1.2). Cluster 2 and Cluster 5 have the density peak near the center point 1 (Fig. 3B).

The pathway enrichment analysis revealed that each cluster has a certain unique biological process. Cluster 1 was formed with 11 proteins (Fig. 3C). Post-translational protein modification was found to be enriched uniquely to cluster 1 (Fig. 3D). Cluster 2 is the larger cluster with 35 proteins, which are primarily involved in the metabolic pathways (glycolysis, pentose phosphate pathway, and glutathione synthesis and recycling pathway) and chaperone mediated autophagic process (Fig. 3E). Cluster 3 was formed with 31 proteins. Several distinct and critical pathways were enriched in Cluster 3, such as cellular response to stress, antigen processing, interleukin signaling, and apoptotic proteins (Fig. 3F). Thirty-three proteins clustered together in the fourth cluster (Fig. 3G). Protein metabolism, formation of cornified envelope, and ECM degradation proteins were present. Cluster 4 showed a negative correlation with Cluster 1, Cluster 2, and Cluster 3. It shows the ECM degradation proteins are inversely proportional to proteins involved in metabolism, PTM of proteins, and FOXO and P53 mediated transcription process. Interestingly, apoptotic proteins were inversely correlated with ECM degradation. Cluster 5 had 22 proteins, and the uniquely enriched pathway was iron uptake and transport. However, as a group, cluster 5 did not show large correlations. (Fig. 3H).

Protein Expression Across Different Grades of KC

The change in protein expression was observed to be more prominent in Grades 2 & 3 of KC against Grade 1 (Fig. 4A and Fig. 4B, respectively). Among the significant differentially expressed proteins, Cystatin S (CST4) and extracellular glycoprotein Lacritin (LACRT) showed significantly higher expression (2.33 ↑, 2.11 ↑ at $P \leq 0.05$) in Grade 2 and (2.14 ↑, 2.97 ↑ at $P \leq 0.05$) in Grade 3 tear fluids compared to patients with Grade 1 KC. LACRT was found to be 1.41↑ in Grade 3 compared to Grade 2; however, it was not statistically significant ($P = 0.11$) (Fig. 4C). These proteins have shown similar trends in expression in Grades 2 and 3 against Controls, as well as geometric means of iTRAQ ratios (CST4- 2.36 ↑ [Grade 2/Con], 2.17 ↑ [Grade 3/Con], LACRT- 1.83 ↑ [Grade 2/Con], 2.58 ↑ [Grade 3/Con]).

Table. List of Differentially Expressed Proteins Across Different KC Grades

		Fold Change			*P* Value		
Gene Symbol	**Protein Name**	**G1/G2**	**G1/G3**	**G2/G3**	**G1 Vs. G2**	**G1 Vs. G3**	**G2 Vs. G3**
ANXA1	Annexin A1	0.57*	0.59*	1.04	0.02‡	0.01‡	0.44
B2M	Beta-2-microglobulin	2.09†	1.98†	0.95	<0.01‡	<0.01‡	0.39
C3	Complement C3	1.81†	1.77†	0.97	0.01‡	0.01‡	0.44
CFL1	Cofilin-1	1.08	1.73†	1.60†	0.28	<0.01‡	<0.01‡
CP	Ceruloplasmin	1.59†	1.54†	0.97	0.01‡	<0.01‡	0.33
CST4	Cystatin-S	2.33†	2.14†	0.92	<0.01‡	<0.01‡	0.45
DMBT1	Deleted in malignant brain tumors 1 protein	2.22†	1.11	0.50*	0.01‡	0.41	<0.01‡
ENO1	Alpha-enolase	0.51*	0.58*	1.15	0.03‡	<0.01‡	0.47
GAPDH	Glyceraldehyde-3-phosphate dehydrogenase	0.73*	1.10	1.52†	0.01‡	0.37	<0.01‡
GSS	Glutathione synthetase	0.64*	0.92	1.43†	0.03‡	0.38	0.07
HSPG2	Basement membrane-specific heparan sulfate proteoglycan core protein	0.63*	0.31*	0.48*	0.08	<0.01	0.01
IGHA1	Immunoglobulin heavy constant alpha 1	1.60†	1.74†	1.08	0.01‡	0.01‡	0.37
IGHG2	Immunoglobulin heavy constant gamma 2	1.92†	2.17†	1.13	0.02‡	<0.01‡	0.26
KRT1	Keratin, type II cytoskeletal 1	0.59*	0.43*	0.73*	0.05‡	<0.01‡	0.09
LACRT	Extracellular glycoprotein lacritin	2.11†	2.97†	1.41†	0.02‡	<0.01‡	0.11
LCN1	Lipocalin-1	0.95	0.50*	0.52*	0.32	0.05‡	0.08
LDHA	L-lactate dehydrogenase A chain	0.52*	0.74*	1.41†	<0.01‡	0.01‡	0.10
LYZ	Lysozyme C	0.90	0.68*	0.76*	0.43	0.21	0.14
PGK1	Phosphoglycerate kinase 1	0.60*	0.62*	1.04	<0.01‡	<0.01‡	0.35
PLA2G2A	Phospholipase A2, membrane associated	0.67*	0.48*	0.72*	0.02‡	<0.01‡	0.18
PPIA	Peptidyl-prolyl cis-trans isomerase A	0.64*	1.03	1.61†	0.03‡	0.35	0.01‡
PSAP	Prosaposin	1.13	0.63*	0.55*	0.37	0.02‡	0.01‡
S100A11	Protein S100-A11	0.71*	2.77†	3.90†	0.29	<0.01‡	<0.01‡
S100A4	Protein S100-A4	1.23†	2.22†	1.81†	0.47	<0.01‡	0.02‡
S100A8	Protein S100-A8	0.89	2.06†	2.33†	0.36	0.01‡	0.01‡
S100A9	Protein S100-A9	0.84	1.69†	2.01†	0.29	0.03‡	0.01‡
S100P	Protein S100-P	1.23†	1.98†	1.61†	0.13	<0.01‡	<0.01‡
SLPI	Antileukoproteinase	1.72†	1.69†	0.98	0.02‡	0.01‡	0.28
SOD1	Superoxide dismutase [Cu-Zn]	0.88	0.60*	0.69*	0.28	<0.01‡	0.02‡
TF	Serotransferrin	1.22†	0.53*	0.44*	0.30	0.01‡	0.01‡
TXN	Thioredoxin	0.90	1.77†	1.96†	0.47	<0.01‡	<0.01‡
WFDC2	WAP four-disulfide core domain protein 2	2.25†	2.69†	1.19	<0.01‡	0.01‡	0.46

* FC < 0.8.
† FC > 1.2.
‡ $P < 0.05$.

Investigative Ophthalmology & Visual Science

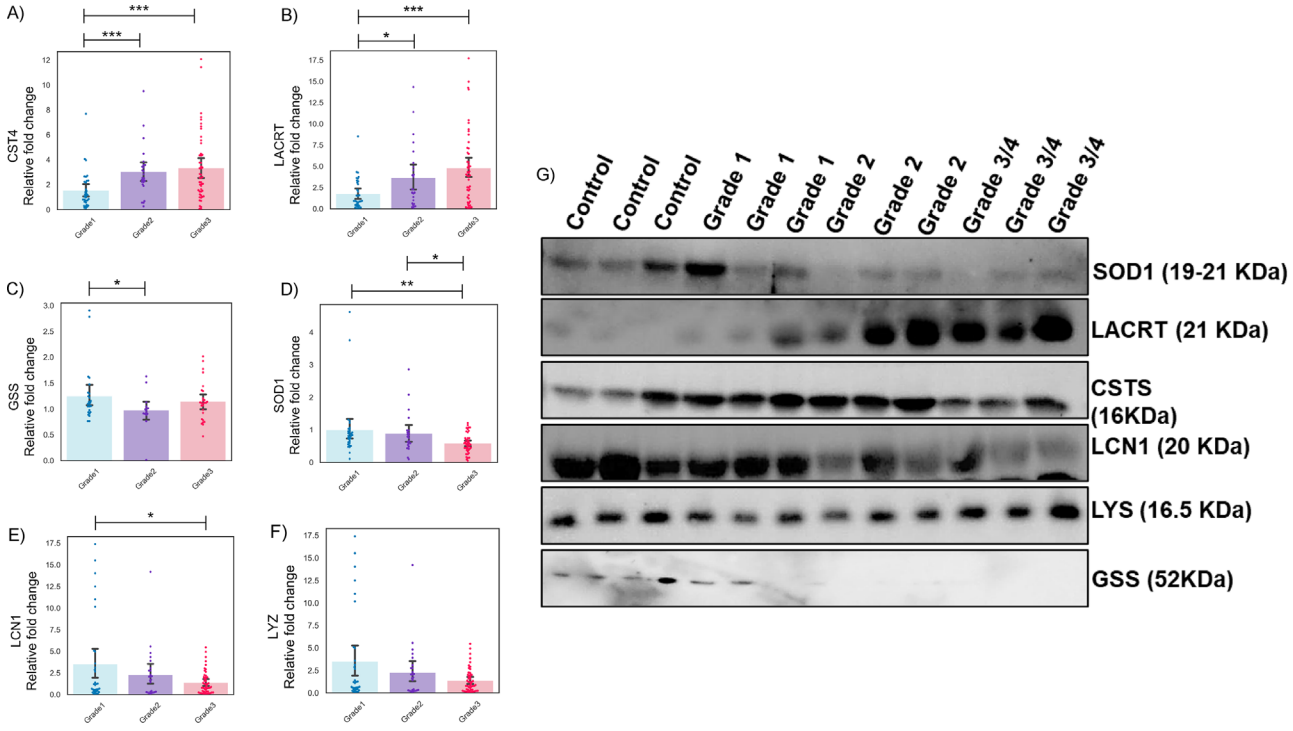

Figure 5. Differentially expressed proteins and validation. **(A–F)** the differential expression of proteins observed for Grade 1, Grade 2, and Grade 3 as compared to the control protein expression level from mass spectrometry values. The Mann-Whitney U-test was used to find the statistical significance of the protein expression among each grade of KC. *$P < 0.05$, **$P < 0.001$, ***$P < 0.001$. **(G)** Immunoblot validation for the key regulatory proteins.

From all the five clusters, 32 proteins were found to be significantly differentially expressed as compared within different grades of KC (Table) with various proportions of dysregulation within each cluster. (Supplementary Fig. S3C). Eight key regulatory processes are found to be altered because of the dysregulated proteins that are involved in glycolytic pathway, protein phosphorylation process, ROS detoxification process, ECM organization, and inflammatory regulatory mechanisms such as adaptive immune system regulation, antigen processing recognition, and neutrophil degranulation (Fig. 4D). Immune regulatory pathways are the major pathways that have a greater number of differentially expression protein levels. Involvement of inflammatory pathways such as adaptive immune system, interleukin signaling, neutrophil degranulation, and antigen processing. The other key pathways such as gluconeogenesis, extracellular matrix organization, and ROS detoxification are also found to be disrupted (Fig. 4E).

Validation of Selected Differentially Regulated Proteins by Western Blotting

Proteins observed to be differentially regulated among the different grades of KC and enriched in functional analysis were selected for further validation. Cystatin S (CST4) is elevated in all grades of KC as compared to the control tear fluids (Fig. 5A). Similarly, the extracellular glycoprotein, Lacritin (LACRT) showed increased expression with the progression of grades from Grade 1 to Grade 3 in comparison with the control (Fig. 5B). Glutathione synthetase (GSS) and superoxide dismutase (SOD1) are the key enzymes that play a major role in maintaining oxidative stress in cells, were found to be down regulated as compared to its controls (Figs. 5C, 5D).

Lipocalin 1 (LCN1) protein expression was found to be lower in tear fluids collected from Grade 3 patients as compared to Grade 1, but we did not observe any difference between Grade 1 and Grade 2 with control (Fig. 5E). Visible differences in protein expression were noticed in Western blot, although it was not significant. There was an increased lysozyme protein expression observed in case of Grade 3 patients as compared to control sample. A very minimal reduction of lysozyme protein expression was observed in case of Grade 1 and Grade 2 patients as compared to the control (Fig. 5F). The western blot shows the different expression patterns for the selected proteins across different grades and controls (Fig. 5G, Supplementary Figs. S4A–F). 1D-SDS PAGE was run for the same set of samples followed by Coomassie blue stain for the total protein normalization (Supplementary Fig. 5A). Densitometry analysis based on the intensity observed in the immunoblotting for each target protein was performed with this total protein normalization, which demonstrated significant changes between control and different grades of KC (Supplementary Figs. 5B–G). A similar trend of protein expression was observed in immunoblotting as compared to mass spectrometry semi-quantification for CST4, LACRT, SOD1, and GSS.

Discussion

Because there remain gaps in understanding the pathogenesis of KC, identifying the clinical grade-wise molecu-

Investigative Ophthalmology & Visual Science

lar changes are critical. The protein dysregulation in tear fluids can be used for diagnosis or monitoring and also could serve as a potential target for therapeutic target. One of the major challenges in tear proteomics is the wide dynamic range of tear proteins. A gel-free approach overcomes such limitations, and, coupled with fractionation methods such as cation exchange chromatography, it aids in resolving sample abundance and complexity. Mass spectrometric analysis for protein biomarkers is advantageous for surveying hitherto unknown proteins, thereby discovering novel molecular changes and quantifying the changes in a multiplexed manner.

The current study identified 1104 proteins from 107 tear fluids of individuals with KC, which is twice the identification as compared to the other untargeted tear proteomics in KC. Out of these, 213 proteins were identified with the observation score > 0.5. Although previously KC was classified as a non-inflammatory disease, recent evidence has changed this status of KC,[50] where increase in proinflammatory cytokines, matrix metalloproteases, and more in tear fluids collected from KC subjects[22,51] have been shown. Other factors like annexin, α1-acid glycoprotein1, and α2-HS glycoprotein, that play a role in inflammation and immune response were found to be dysregulated in our data and supported by previous observations.[43] The biological processes of the identified proteins in the present study were found to be involved in inflammation, oxidative stress response, and regulation of apoptosis, which agree with various experimental studies proposing the involvement of these pathways in KC. Interestingly, our dataset further reveals the disruption of metabolic pathways such as glycolytic pathway, glutathione synthesis pathway, and pentose phosphate pathway.

Proteins with an observation rate >0.5 that were present in tear fluids from all the grades formed five different clusters (based on the Euclidean distance between each protein), each of which possessed unique functional enrichments. Interestingly, ECM degradation proteins (cluster 4) show an inverse correlation with the proteins involved in metabolic pathways, detoxification of ROS, and cellular response to stress. The 22 proteins of cluster 5 were unique from each other and did not group with other clusters; however, they show altered iron uptake, which is pathologic in KC, a feature that had never been demonstrated in tear analyses.[52,53]

The progression of KC has been proposed to be associated with metabolic factors, as well as inflammatory mediators, hormones, metabolites, and micronutrients.[12] Glycolysis is one of the major metabolic processes that produces energy and critical for cell survival. GAPDH, ENO1, and PGK1 are the key components of glycolysis pathway. We identified these proteins in tear fluids and found them to be significantly downregulated in Grade 1 KC as compared to control suggestive of a metabolic dysfunction early in the disease. In higher grades of KC, a gradual increase in expression for these enzymes could be observed, which may be a reactive response of the tissue as the ectatic process continues. Metabolic imbalances in cornea could lead to an increased lactate production.[54,55] Abundant lactate synthesis could increase oxidative stress by lowering the extracellular pH and increase apoptosis of keratocytes and epithelial cells, which may be a mechanism driving the loss of cells observed in KC eyes. We observed increased expression of proteins such as S100A8 and S100A9 that are indicative of, and can themselves promote, apoptosis in KC eyes.

A significant decrease in the expression of both GSS and SOD was observed across the KC grades GSS and SOD1 are crucial enzymes in the cellular antioxidant defense system.[56] The SOD1 expression level was reduced as the disease progressed from Grade 1 to Grade 3, where Grade 3 had the lowest expression level and was validated by direct immunoblotting from patient tears. The pathological role of oxidative stress in KC is reported, wherein proteins like serum albumin, hemopexin, heat shock cognate 71kDa, and iron binding proteins involved in managing oxidative stress were downregulated.[43] Taken together with our dataset, the involvement of metabolic imbalance could be one of the reasons for oxidative stress due to higher lactate production. We observed a strong inverse correlation between ECM organization and NK cell activation through MHC-class I antigen processing. Four proteins among the dysregulated proteins (HSPG2, lysozyme, MIF, and KNG1) were found to be involved in immunological process as demonstrated by previous studies.[5] Our study identified novel proteins, which indicates the metabolic imbalance and immunoinflammatory response in KC across various grades. These targets could serve as novel therapeutic targets for KC. Despite the large number of proteins discovered in this cohort that expands the disease associated protein repertoire, some critical limitations remain. Some of the proteins related to pathogenesis of KC such as cytokines, MMPs, LOX, collagens, and more, which are detectable by antibody-based assays are poorly identified in mass spectrometric analyses due to the inherent technical challenges. The soluble factors such as MMP9, MMP2, and TNFα were identified among many other proteins through LegendPLEX in tear fluids of KC patients.[5] Although collagens and regulatory proteins like LOX are not detectable in the LC-MS process, proteins that positively regulate collagen fibril formation such as ANXA2, CTSB, and FMOD and negative regulators of collagen fibril formation such as TIMP1 and CTS3 were detected in this study. Low abundance proteins are difficult to detect since their digested peptides are masked by high abundance ones. Secondly, while many different proteins have been identified, it is challenging to perform validation tests for all due to the relatively low amounts of protein available for techniques such as western blotting from individual patients. Individual variable dependent sample size estimations have the limitation of being underpowered. However, the findings in the study hold strong evidence for the significant changes through mass spectrometry. This shows that the sample size estimation was not biased by the chosen factor. It should also be noted that high-throughput techniques such as LC-MS/MS are cost, time, and labor intensive; therefore performing such techniques at a scale like population genetics is not feasible with the currently available technologies.

Conclusions

We discovered a number of novel dysregulated processes and proteins in KC eyes. These have implications for developing disease stage specific tear biomarkers, as well as potential targets for therapeutic intervention. We found that LACRT and CST4 showed significant increases in expression levels across grades. However, these proteins remain unchanged in Grade 1 compared to control, which establishes them as ideal candidate markers for tracing the progression of early grades of KC in tear fluids with respect to Grade 1/Grade 2, Grade 1/Grade 3, and Grade 2/Grade 3. Also, the proteins involved in the ECM organization,

Investigative Ophthalmology & Visual Science

inflammatory modulatory action, ROS detoxification, and metabolic pathways were found to be dysregulated. Our unbiased proteomics study unveiled a plausible mechanism underlying KC disease pathogenesis.

Acknowledgments

The authors thank the Late Roger Bueurman, Sharon D'Souza, Late K Bhujang Shetty for their support and guidance. AG and RS thank Narayana Nethralaya Foundation and DST-SERB (EMR/2016/003624) for the funding support. LZ thanks InnoHK initiative and the Hong Kong Special Administrative Region Government for their support.

Disclosure: **R. Kannan**, None; **R. Shetty**, None; **T. Panigrahi**, None; **S.K. Koh**, None; **P. Khamar**, None; **V. Deshpande**, None; **R.M.M.A. Nuijts**, None; **M. Gijs**, None; **K. Nishtala**, None; **L. Zhou**, None; **A. Ghosh**, None

References

1. Rabinowitz YS. Keratoconus. *Surv Ophthalmol*. 1998;42:297–319.
2. Belin MW, Jang HS, Borgstrom M. Keratoconus: diagnosis and staging. *Cornea*. 2022;41:1–11.
3. Santodomingo-Rubido J, Carracedo G, Suzaki A, Villa-Collar C, Vincent SJ, Wolffsohn JS. Keratoconus: an updated review. *Contact Lens Anterior Eye*. 2022;45(3):101559.
4. Munir SZ, Munir WM, Albrecht J. Estimated prevalence of keratoconus in the United States from a large vision insurance database. *Eye Contact Lens*. 2021;47:505–510.
5. D'Souza S, Nair AP, Sahu GR, et al. Keratoconus patients exhibit a distinct ocular surface immune cell and inflammatory profile. *Sci Rep*. 2021;11:1–16.
6. Gijs M, Adelaar TI, Vergouwen DP, et al. Tear fluid inflammatory proteome analysis highlights similarities between keratoconus and allergic conjunctivitis. *Invest Ophthalmol Vis Sci*. 2023;64:9–9.
7. Khaled ML, Helwa I, Drewry M, Seremwe M, Estes A, Liu Y. Molecular and histopathological changes associated with keratoconus. *BioMed Res Int*. 2017;2017(1):7803029.
8. Yam GH-F, Fuest M, Zhou L, et al. Differential epithelial and stromal protein profiles in cone and non-cone regions of keratoconus corneas. *Sci Rep*. 2019;9:1–17.
9. Blackburn BJ, Jenkins MW, Rollins AM, Dupps WJ. A review of structural and biomechanical changes in the cornea in aging, disease, and photochemical crosslinking. *Front Bioeng Biotechnol*. 2019;7:66.
10. Sherwin T, Brookes N, Loh I-P, Poole C, Clover G. Cellular incursion into Bowman's membrane in the peripheral cone of the keratoconic cornea. *Exp Eye Res*. 2002;74:473–482.
11. White TL, Lewis PN, Young RD, et al. Elastic microfibril distribution in the cornea: Differences between normal and keratoconic stroma. *Exp Eye Res*. 2017;159:40–48.
12. Shetty R, D'Souza S, Khamar P, Ghosh A, Nuijts RM, Sethu S. Biochemical markers and alterations in keratoconus. *Asia Pac J Ophthalmol*. 2020;9:533–540.
13. Shetty R, Sathyanarayanamoorthy A, Ramachandra RA, et al. Attenuation of lysyl oxidase and collagen gene expression in keratoconus patient corneal epithelium corresponds to disease severity. *Mol Vis*. 2015;21:12.
14. Dudakova L, Liskova P, Trojek T, Palos M, Kalasova S, Jirsova K. Changes in lysyl oxidase (LOX) distribution and its decreased activity in keratoconus corneas. *Exp Eye Res*. 2012;104:74–81.
15. Dudakova L, Sasaki T, Liskova P, Palos M, Jirsova K. The presence of lysyl oxidase-like enzymes in human control and keratoconic corneas. *Histol Histopathol*. 2016;31:63–71.
16. Ghosh A, Jeyabalan N, Shetty R, Mohan RR. Keratoconus in Asia. In: Prakash G, Iwata T, (eds). *Advances in Vision Research, Volume I: Genetic Eye Research in Asia and the Pacific*. Tokyo: Springer; 2017;363–374.
17. Balasubramanian SA, Mohan S, Pye DC, Willcox MDP. Proteases, proteolysis and inflammatory molecules in the tears of people with keratoconus. *Acta Ophthalmol*. 2012;90:e303–e309.
18. García B, García-Suárez O, Merayo-Lloves J, et al. Heparanase overexpresses in keratoconic cornea and tears depending on the pathologic grade. *Dis Markers*. 2017;2017:3502386.
19. Smith V, Rishmawi H, Hussein H, Easty D. Tear film MMP accumulation and corneal disease. *Br J Ophthalmol*. 2001;85:147–153.
20. Zhou L, Sawaguchi S, Twining SS, Sugar J, Feder RS, Yue B. Expression of degradative enzymes and protease inhibitors in corneas with keratoconus. *Invest Ophthalmol Vis Sci*. 1998;39:1117–1124.
21. Pahuja N, Kumar NR, Shroff R, et al. Differential molecular expression of extracellular matrix and inflammatory genes at the corneal cone apex drives focal weakening in keratoconus. *Invest Ophthalmol Vis Sci*. 2016;57:5372–5382.
22. Shetty R, Ghosh A, Lim RR, et al. Elevated expression of matrix metalloproteinase-9 and inflammatory cytokines in keratoconus patients is inhibited by cyclosporine A. *Invest Ophthalmol Vis Sci*. 2015;56:738–750.
23. Whitelock RB, Fukuchi T, Zhou L, et al. Cathepsin G, acid phosphatase, and alpha 1-proteinase inhibitor messenger RNA levels in keratoconus corneas. *Invest Ophthalmol Vis Sci*. 1997;38:529–534.
24. Sawaguchi S, Twining SS, Yue B, et al. Alpha 2-macroglobulin levels in normal human and keratoconus corneas. *Invest Ophthalmol Vis Sci*. 1994;35:4008–4014.
25. Joseph R, Srivastava O, Pfister R. Differential epithelial and stromal protein profiles in keratoconus and normal human corneas. *Exp Eye Res*. 2011;92:282–298.
26. Behndig A, Karlsson K, Johansson BO, Brännström T, Marklund SL. Superoxide dismutase isoenzymes in the normal and diseased human cornea. *Invest Ophthalmol Vis Sci*. 2001;42:2293–2296.
27. Shetty R, Sharma A, Pahuja N, et al. Oxidative stress induces dysregulated autophagy in corneal epithelium of keratoconus patients. *PloS One*. 2017;12:e0184628.
28. Saijyothi AV, Fowjana J, Madhumathi S, et al. Tear fluid small molecular antioxidants profiling shows lowered glutathione in keratoconus. *Exp Eye Res*. 2012;103:41–46.
29. Lackner E-M, Matthaei M, Meng H, Ardjomand N, Eberhart CG, Jun AS. Design and analysis of keratoconus tissue microarrays. *Cornea*. 2014;33:49–55.
30. Toprak I, Kucukatay V, Yildirim C, Kilic-Toprak E, Kilic-Erkek O. Increased systemic oxidative stress in patients with keratoconus. *Eye*. 2014;28:285–289.
31. Caglayan M, Kocamıs SI, Sarac O, et al. Investigation of heme oxygenase 2 enzyme protein expression in keratoconus and normal human corneal epithelium: an immunohistochemical study. *Curr Eye Res*. 2019;44:25–29.
32. Atilano SR, Lee DH, Fukuhara PS, et al. Corneal oxidative damage in keratoconus cells due to decreased oxidant elimination from modified expression levels of SOD enzymes, PRDX6, SCARA3, CPSF3, and FOXM1. *J Ophthalmic Vis Res*. 2019;14:62.
33. Zhou L, Yue BY, Twining SS, Sugar J, Feder RS. Expression of wound healing and stress-related proteins in keratoconus corneas. *Curr Eye Res*. 1996;15:1124–1131.

34. Gondhowiardjo TD, van Haeringen NJ. Corneal aldehyde dehydrogenase, glutathione reductase, and glutathione S-transferase in pathologic corneas. *Cornea*. 1993;12:310–314.
35. und Hohenstein-Blaul NVT, Funke S, Grus FH. Tears as a source of biomarkers for ocular and systemic diseases. *Exp Eye Res*. 2013;117:126–137.
36. Nishtala K, Pahuja N, Shetty R, Nuijts RM, Ghosh A. Tear biomarkers for keratoconus. *Eye Vis*. 2016;3:1–7.
37. Zhou L, Beuerman RW. Tear analysis in ocular surface diseases. *Prog Retin Eye Res*. 2012;31:527–550.
38. Lema I, Brea D, Rodríguez-González R, Díez-Feijoo E, Sobrino T. Proteomic analysis of the tear film in patients with keratoconus. *Mol Vis*. 2010;16:2055.
39. Goñi N, Martínez-Soroa I, Ibarrondo O, et al. Tear proteome profile in eyes with keratoconus after intracorneal ring segment implantation or corneal crosslinking. *Front Med (Lausanne)*. 2022;9:944504.
40. Yenihayat F, Altıntaş Ö, Kasap M, Akpınar G, Güzel N, Çelik OS. Comparative proteome analysis of the tear samples in patients with low-grade keratoconus. *Int Ophthalmol*. 2018;38:1895–1905.
41. López-López M, Regueiro U, Bravo SB, et al. Shotgun proteomics for the identification and profiling of the tear proteome of keratoconus patients. *Invest Ophthalmol Vis Sci*. 2022;63:12–12.
42. Balasubramanian SA, Wasinger VC, Pye DC, Willcox MD. Preliminary identification of differentially expressed tear proteins in keratoconus. *Mol Vis*. 2013;19:2124.
43. López-López M, Regueiro U, Bravo SB, et al. Tear proteomics in keratoconus: A quantitative SWATH-MS analysis. *Invest Ophthalmol Vis Sci*. 2021;62:30–30.
44. de Almeida Borges D, Alborghetti MR, Franco Paes Leme A, et al. Tear proteomic profile in three distinct ocular surface diseases: keratoconus, pterygium, and dry eye related to graft-versus-host disease. *Clin Proteomics*. 2020;17:1–16.
45. Pannebaker C, Chandler HL, Nichols JJ. Tear proteomics in keratoconus. *Mol Vis*. 2010;16:1949.
46. Acera A, Vecino E, Rodríguez-Agirretxe I, et al. Changes in tear protein profile in keratoconus disease. *Eye*. 2011;25:1225–1233.
47. Ghosh A, Zhou L, Ghosh A, Shetty R, Beuerman R. Proteomic and gene expression patterns of keratoconus. *Indian J Ophthalmol*. 2013;61:389.
48. Ishii R, Kamiya K, Igarashi A, Shimizu K, Utsumi Y, Kumanomido T. Correlation of corneal elevation with severity of keratoconus by means of anterior and posterior topographic analysis. *Cornea*. 2012;31:253–258.
49. Mihaltz K, Kovacs I, Takacs A, Nagy ZZ. Evaluation of keratometric, pachymetric, and elevation parameters of keratoconic corneas with pentacam. *Cornea*. 2009;28:976–980.
50. Shetty R, Khamar P, Kundu G, Ghosh A, Sethu S. Inflammation in keratoconus. In: Izquierdo L, Henriquez M, Mannis M, eds. *Keratoconus*. Philadelphia: Elsevier; 2023:159–168.
51. Lema I, Sobrino T, Duran JA, Brea D, Diez-Feijoo E. Subclinical keratoconus and inflammatory molecules from tears. *Br J Ophthalmol*. 2009;93:820–824.
52. Hiratsuka Y, Nakayasu K, Kanai A. Secondary keratoconus with corneal epithelial iron ring similar to Fleischer's ring. *Jpn J Ophthalmol*. 2000;44:381–386.
53. Bamdad S, Owji N, Bolkheir A. Association between advanced keratoconus and serum levels of zinc, calcium, magnesium, iron, copper, and selenium. *Cornea*. 2018;37:1306–1310.
54. McKay TB, Hjortdal J, Sejersen H, Asara JM, Wu J, Karamichos D. Endocrine and metabolic pathways linked to keratoconus: implications for the role of hormones in the stromal microenvironment. *Sci Rep*. 2016;6:25534.
55. Sharif R, Sejersen H, Frank G, Hjortdal J, Karamichos D. Effects of collagen cross-linking on the keratoconus metabolic network. *Eye (Lond)*. 2018;32:1271–1281.
56. Pigeolet E, Corbisier P, Houbion A, et al. Glutathione peroxidase, superoxide dismutase, and catalase inactivation by peroxides and oxygen derived free radicals. *Mech Ageing Dev*. 1990;51:283–297.

Investigative Ophthalmology & Visual Science